

Robust and Efficient Writer-Independent IMU-Based Handwriting Recognition

Jindong Li¹[0000-0002-3550-1660], Tim Hamann²[0000-0003-3562-6882], Jens Barth²[0000-0003-3967-9578], Peter Kämpf², Dario Zanca¹[0000-0001-5886-0597],
and Björn Eskofier¹[0000-0002-0417-0336]

¹ Machine Learning and Data Analytics Lab, Friedrich-Alexander-Universität
Erlangen-Nürnberg, Germany
² STABILO International GmbH, Germany

Abstract. Online handwriting recognition (HWR) using data from inertial measurement units (IMUs) remains challenging due to variations in writing styles and the limited availability of annotated datasets. Previous approaches often struggle with handwriting from unseen writers, making writer-independent (WI) recognition a crucial yet difficult problem. This paper presents an HWR model designed to improve WI HWR on IMU data, using a CNN encoder and a BiLSTM-based decoder. Our approach demonstrates strong robustness to unseen handwriting styles, outperforming existing methods on the WI splits of both the public OnHW dataset and our word-based dataset, achieving character error rates (CERs) of 7.37% and 9.44%, and word error rates (WERs) of 15.12% and 32.17%, respectively. Robustness evaluation shows that our model maintains superior accuracy across different age groups, and knowledge learned from one group generalizes better to another. Evaluation on our sentence-based dataset further demonstrates its potential in recognizing full sentences. Through comprehensive ablation studies, we show that our design choices lead to a strong balance between performance and efficiency. These findings support the development of more adaptable and scalable HWR systems for real-world applications. The code is available at: <https://github.com/jindongli24/REWI>.

Keywords: Online Handwriting Recognition · Time-series Analysis · Inertial Measurement Unit

1 Introduction

Handwriting has long been a primary means of recording and sharing information throughout human history. With advancements in technology, the demand for digitizing handwritten content has increased. HWR, which converts handwritten symbols into computer-readable text, has become an important area of research.

Offline HWR, as one of the main types of HWR, has been widely used in everyday applications and various research fields, including historical studies [16] and healthcare [6]. However, it is limited to recognizing static images of handwritten text. In contrast, online HWR processes time-series data that captures

dynamic handwriting features such as strokes, positions, directions, and velocities. This data is typically collected using touchscreens and styluses on mobile devices [2], which limits the available writing surface for users.

Another approach to online HWR uses pens equipped with IMUs [20,1,13]. These sensors capture pen movements without relying on the exact position of the tip, allowing the pen to operate independently of external devices and on virtually any surface, demonstrating strong potential for online HWR applications. However, variations in handwriting styles can still affect recognition accuracy, and sensor noise from rough surfaces, temperature changes, and digitization artifacts presents additional challenges.

This paper presents a sequence-to-sequence model for IMU-based online HWR, designed to address challenges arising from handwriting style variations and sensor noise. The model adopts an encoder-decoder architecture, combining a convolutional neural network (CNN) with a bidirectional long short-term memory (BiLSTM) network. It also incorporates recent advancements in deep learning by using customized convolutional layers. We evaluate the proposed model by benchmarking it against several existing IMU-based HWR methods, as well as adapted mainstream models that have achieved strong performance in various deep learning tasks. The evaluation is conducted on datasets collected using an IMU-based pen, each capturing different aspects of the problem space. Experimental results demonstrate that our model outperforms others in terms of efficiency, robustness, and flexibility in WI HWR.

2 Related Works

2.1 IMU-based HWR

IMU-based HWR has been an active area of research for decades. Early studies, such as [3,8], employed DTW-based algorithms to recognize digit data collected with IMU-based pens, achieving recognition rates above 90%. Later works, including [12,13], explored LSTM-based models for recognizing individual English characters, reporting recognition accuracies of up to 99.68% and 79.01% on their respective datasets. Although these methods achieved high accuracy, they rely on isolated character recognition, processing entire input sequences to classify single characters. This character-by-character approach disrupts the natural writing flow, making it less practical for real-world applications where writing typically occurs word by word.

To address more complex tasks, [21,14] employed CNN-BiLSTM models with connectionist temporal classification (CTC) [5] to recognize sequences of English and German characters. These models were evaluated on datasets collected using the IMU-based pen developed by STABILO. Although they achieved CERs of 27.8% and 17.97%, which are higher than those of earlier approaches, they marked an important step toward recognizing full words and even sentences, moving closer to practical applications.

2.2 Advancements in Deep Learning Architectures

In recent years, the introduction of ResNet [7] and Transformers [19] has significantly advanced the development of deep learning models. ResNet addressed the vanishing gradient problem through skip connections, enabling the effective training of very deep neural networks. Transformers introduced self-attention mechanisms, which improved parallelization and enhanced the modeling of long-range dependencies compared to CNN or recurrent neural networks.

Building on these innovations, several new approaches have been proposed. MLP-Mixer [18] demonstrated that strong performance in vision tasks can be achieved without convolutions or self-attention, relying solely on multi-layer perceptrons to mix spatial and channel information. Swin Transformers [10,9] introduced a hierarchical architecture with shifted window-based self-attention, enabling efficient multi-scale modeling for various vision tasks. ViT [4] treats an image as a sequence of patch embeddings fed into a Transformer encoder, showing that pure self-attention rivals CNNs on large-scale vision tasks. ConvNeXt [11] integrated concepts from both CNNs and Transformers, achieving state-of-the-art performance while preserving the simplicity and efficiency of traditional CNNs.

Although these models were originally designed for different tasks, their core principles, such as self-attention and hierarchical structures, are potentially well-suited for time-series data. Applying these techniques to IMU-based HWR could enhance performance and open new research opportunities in the field.

3 Methods

3.1 Model Architecture

CLDNN [21] demonstrated a promising approach to word-level HWR, achieving solid performance while still leaving room for improvement. Building on CLDNN, we designed our model by incorporating recent advancements in CNN architecture to improve both efficiency and robustness, as illustrated in Fig. 1. The CNN encoder efficiently extracts and embeds input features, while the BiLSTM decoder captures contextual information in both forward and backward temporal directions. Both the CNN and BiLSTM are capable of handling inputs of varying lengths, providing flexibility for different types of handwriting data.

The encoder has three stages, each consisting of an embedding layer followed by three convolutional blocks. The embedding layer uses a convolutional layer with a kernel size of 2 and a stride of 2 to downsample the input sequences, followed by an instance normalization layer. Except for in the first stage, which takes inputs with 13 channels, the embedding layers double the number of output channels relative to the number of input channels.

The design of the convolutional block is inspired by recent works like ConvNeXt. To reduce computational cost while maintaining comparable performance, each block employs depthwise-dilated separable convolutional layers. This design first applies a grouped convolutional layer with a kernel size of 5

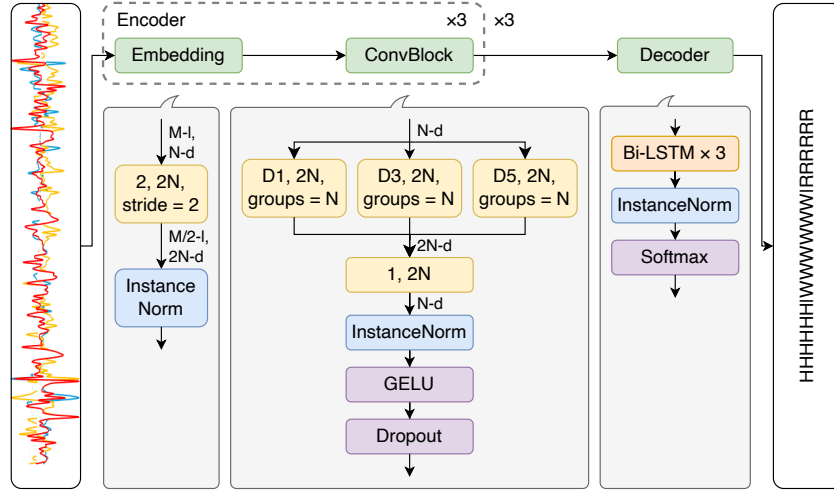


Fig. 1. Model architecture. The model consists of a three-stage CNN encoder and a BiLSTM-based decoder. The convolutional blocks use depthwise-dilated separable convolutional layers with varying kernel sizes to capture multi-scale features, while doubling the number of output channels to create a larger hidden space for the pixelwise convolutional layer to operate effectively.

that doubles the number of channels, where the number of groups is equal to the number of input channels. This is followed by a 1D pixelwise convolution that reduces the number of channels back to the original. Compared to standard depthwise separable convolutions, this structure creates a larger hidden space for improved feature representation while still consuming fewer computational resources than a standard convolutional layer.

In addition to the depthwise-dilated separable convolution, we introduce a multi-scale convolutional design, which adds two more convolutional layers with smaller kernel sizes of 1 and 3. The input sequence is processed in parallel by these three convolutional layers, and the outputs are summed before being passed to the pixelwise convolutional layers. After training, the weights of the smaller-kernel convolutional layers are merged into the layer with the kernel size of 5, resulting in the same number of parameters as a standard depthwise-dilated separable convolution. This approach enables learning multi-scale features during training without adding extra parameters or computational cost during inference. Each multi-scale depthwise-dilated separable convolution is followed by a 1D instance normalization layer, a GELU activation function, and a dropout layer with a drop rate of 0.2.

The decoder consists of three BiLSTM layers, each with a hidden size of 128 and a dropout rate of 0.2. These layers are followed by a fully connected layer and a Softmax layer for timestep-wise classification, omitting the intermediate

hidden layers used in CLDNN to enhance efficiency. The Softmax outputs are then processed by a greedy CTC decoder to generate the final predictions.

To better support edge computing, we also introduce a lightweight version of the model, which reduces the embedded channel sizes from 128, 256, and 512 to 64, 128, and 256. The BiLSTM decoder is also shrunk, with the hidden size reduced to 64 and the number of layers reduced to 2.

3.2 Data Augmentation

To enhance robustness against noise and diverse handwriting styles, we applied four data augmentation techniques: AddNoise, Drift, Dropout, and TimeWarp. Each technique has a 25% probability of being applied to a given signal. TimeWarp affects only the time dimension, while the other methods are applied multiplicatively to ensure their contributions are not overshadowed by the magnitude of the original signals. Visualizations of all data augmentation methods are provided in Appendix A. After augmentation, all signals are normalized.

AddNoise adds Gaussian noise to the original signals. **Drift** divides the signals into segments and applies random drift within each segment. **Dropout** randomly replaces small segments of the signal with the last value preceding each segment. **TimeWarp** randomly adjusts the speed of segments of the original signal.

3.3 Datasets

Private Dataset Our datasets were collected using the IMU-based pen developed by STABLO, as shown in Figure 2. The pen is equipped with two accelerometers (one at each end), a gyroscope, a magnetometer, and a force sensor. These sensors generate 13 output channels at a sampling rate of 400 Hz or 100Hz. Each sensor provides three channels of data, except for the force sensor, which provides a single channel.

We first collected a dataset consisting of 1,547 recording sessions with participants of different ages and handedness, resulting in 24,163 samples of English and German words of varying lengths. These words span 59 character categories, including both uppercase and lowercase letters from both languages. The data samples were downsampled to 100 Hz where necessary, and only those shorter than 1,024 time steps were retained. Additionally, we collected another dataset consisting of 1,547 recording sessions with participants of different ages and handedness, resulting in 20,639 samples of English and German sentences. These sentences span 84 character categories, including uppercase and lowercase letters from both languages, as well as numbers, symbols, and spaces. The data samples were also downsampled to 100 Hz where necessary, and only those shorter than 4,096 time steps were retained.

After preprocessing, the data samples are split into a training set (80%) and a validation set (20%) using 5-fold cross-validation. Two splitting configurations are used: WI and random. In the WI split, the data are divided at the writer level, ensuring that no writer appears in both the training and validation sets,

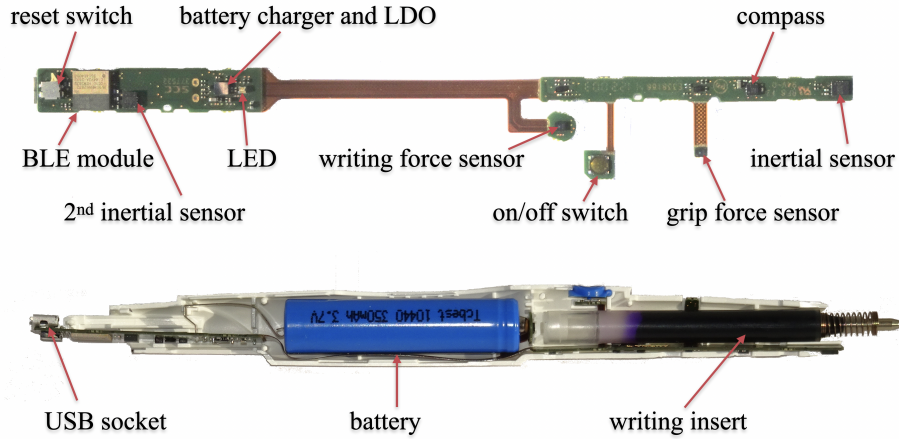


Fig. 2. Digipen Architecture. The pen includes two IMUs (one with an accelerometer and gyroscope, the other with only an accelerometer) located at both ends, a magnetometer (compass), a writing force sensor, and a grip force sensor (not used in the experiments).

thereby keeping handwriting styles independent. In the random split, samples are assigned without regard to writer identity. Notably, the sentence-based dataset is split only using the WI configuration.

To evaluate the robustness of the system, we also analyze subsets of the WI dataset based on participants' ages. Since children are still developing their handwriting skills, their handwriting patterns differ significantly from those of adults, particularly in writing speed and discontinuity due to high cognitive load, typically stabilizing around 14 years old [15,17]. Based on this, we classify participants aged 12 and under as children to ensure that most writers represent typical children's handwriting patterns, and those aged 18 and older as adults. Data from participants aged 13 to 17 are excluded from these subsets because some have already developed mature and fluent handwriting, making them less representative of either the children or adult groups. Notably, the adult subset (13,899 samples) is approximately twice the size of the children subset (7,762 samples).

OnHW Dataset For commercial reasons, our private dataset will not be made publicly available. However, we also use two splits from the right-handed subset of the public OnHW-words500 dataset [14], which contains IMU-based handwriting data for 500 words written by 53 writers: a writer-dependent (WD) subset, divided by words, and a WI subset. Due to the small size of the left-handed subset (only 1,000 samples) and its limited split configuration (only two splits: one for training and one for validation), it is excluded from our experiments.

4 Experiments

The experiments consist of five parts: evaluation on our word-based dataset, evaluation on the OnHW datasets, robustness evaluation, evaluation on our sentence-based dataset, and an ablation study. In each part, models are trained using 5-fold cross-validation, and the best result from each fold’s validation set is used to calculate the average across the five folds, which is reported as the final result.

We first include two previous works: CNN+BiLSTM [14] and CLDNN [21]. Since their code is not publicly available, we re-implemented both in PyTorch based on the original papers. For CLDNN, we followed the described training and preprocessing pipeline. However, training details for CNN+BiLSTM were not clearly specified, so we trained it using our own pipeline to ensure a fair comparison. These two models are compared with the small version of our model, given their similar sizes.

For broader comparison, we implemented ResNet, MLP-Mixer, ViT, ConvNeXt, and Swin Transformer V2 backbones as encoders, replacing the CNN encoder in the base version of our model. Since these backbones were originally designed for images, we modified them to handle time-series input. Due to architectural limitations, MLP-Mixer, ViT, and Swin Transformer V2 require fixed-size inputs. Therefore, input sequences are zero-padded to a length of 1,024 for these models. Additionally, encoders and decoders are configured with hyperparameters to ensure a comparable number of parameters when using 1,024-length input sequences. Given their model sizes, these approaches are compared against the base version of our model.

Except for CLDNN [21], which is trained as described in its original paper, all other models are trained using the same procedure. We use the AdamW optimizer with a learning rate of 0.001 for 300 epochs. To improve training stability and convergence, a linear learning rate warm-up is applied, starting at 0.0001 for the first 30 epochs, followed by a cosine annealing schedule for the remaining epochs. The training process uses the CTC loss function and a batch size of 64. Models are checkpointed and evaluated every 5 epochs during training.

To measure model performance, we use two metrics: CER and WER. These measure how many errors appear in the model’s predictions, including substitutions, deletions, and insertions, compared to the total number of characters or words in the correct text. CER reflects errors at the character level, while WER reflects errors at the word level. We also evaluate memory usage and computational cost by reporting the number of parameters (#Params) and the number of multiply and accumulate operations (MACs). These are calculated using a random input sequence with 13 channels and 1,024 timesteps for the word-based datasets, and 4,096 timesteps for the sentence-based dataset.

4.1 Evaluation on Our Word-Based Dataset

In this section, we compare our models with other approaches using the random and WI splits of our word-based dataset.

Table 1. Results on Our Word-Based Dataset. We compare our models with other approaches on the random and WI splits of our word-based dataset. Metrics include CER, WER, #Params, and MACs, which measure computational cost. Error rates are reported as percentages. The best results are shown in **bold**.

Models	Random		WI		#Params	MACs
	CER	WER	CER	WER		
CLDNN [21]	15.52	53.62	19.05	60.20	0.75M	291M
CNN+BiLSTM [14]	16.24	56.13	21.32	64.83	0.40M	152M
Ours-S	11.47	42.64	15.29	50.70	0.53M	79M
ResNet [7] (enc.)	7.51	28.58	10.89	36.71	3.97M	591M
MLP-Mixer [18] (enc.)	8.53	32.36	16.30	50.89	3.90M	802M
ViT [4] (enc.)	9.77	36.50	13.89	45.24	3.71M	477M
ConvNeXt [11] (enc.)	8.17	32.51	12.25	42.16	3.86M	600M
SwinV2 [9] (enc.)	7.93	31.78	11.70	40.69	3.88M	601M
Ours-B	6.88	26.06	9.44	32.17	3.89M	600M

As shown in Table 1, in comparison with other IMU-based HWR approaches, the small version of our model outperforms all others in both CER and WER on the random split (11.47% and 42.64%) and the WI split (15.29% and 50.70%), while maintaining the lowest computational cost. The second-best approach, CLDNN, performs 35.3% and 25.8% worse in CER and WER on the random split, and 24.6% and 18.7% worse on the WI split, compared to the small version of our model. Moreover, its number of parameters and computational cost are 43.4% and 268% higher, respectively.

Compared to other mainstream models, the base version of our model still achieves the lowest CER and WER on the random split (6.88% and 26.06%) and the WI split (9.44% and 32.17%). ResNet achieves the second lowest error rates, 7.51% CER and 28.58% WER on the random split and 10.89% CER and 36.71% WER on the WI split. Unlike backbones that prefer local attention like Swin Transformer V2 and CNNs, backbones focusing on global information like Vision Transformer and MLP-Mixer performs the worst across all metrics.

Additionally, we investigate the errors made by the base version of our model on the WI split of our word-based dataset. As shown in Appendix C, substitution is the primary error type. Most of these substitution errors result from confusion between uppercase and lowercase letters with similar patterns, such as "c" and "w". However, there are also instances of confusion between different letters with similar shapes, such as "q" and "g".

4.2 Evaluation on the OnHW Dataset

In this section, we compare our models with other approaches using the WD and WI splits of the right-handed subset of the OnHW dataset. All models are trained and evaluated following the same procedure described in the previous

section. For reference, we also include the published results for CNN+BiLSTM on the OnHW dataset.

Table 2. Results on the Right-Handed Subset of the OnHW Dataset. We compare our models with other approaches on the WD and WI splits of the OnHW dataset.

Models	WD		WI	
	CER	WER	CER	WER
CLDNN	16.18	50.98	15.62	36.71
CNN+BiLSTM (orig.)	17.16	51.95	27.80	60.91
CNN+BiLSTM	15.47	51.55	17.66	43.45
Ours-S	15.73	50.64	10.55	24.94
ResNet (enc.)	12.72	40.76	8.22	18.35
MLP-Mixer (enc.)	14.74	46.89	9.74	21.87
ViT (enc.)	17.86	52.00	10.49	22.71
ConvNeXt (enc.)	14.66	45.42	8.23	18.46
SwinV2 (enc.)	13.23	43.72	8.62	19.60
Ours-B	14.43	43.90	7.37	15.12

As shown in Table 2, the small version of our model achieves the lowest error rates on the WI split, with a CER of 10.55% and a WER of 24.94%. Although CNN+BiLSTM has the lowest CER of 15.47% on the WD split of the OnHW dataset, the small version of our model achieves the best WER at 50.64%. By comparing the CER and WER from the original paper with those from our re-implementation, it is also evident that simply applying our training pipeline and data augmentations leads to significant performance improvements, especially on the WI split, where the CER and WER improve by 36.5% and 28.7%, respectively.

Compared to other mainstream models, the base version of our model again achieves the best performance on the WI split, with a CER of 7.37% and a WER of 15.12%. However, ResNet performs best on the WD split, with a CER of 12.72% and a WER of 40.73%. Global attention-based backbones consistently perform the worst across all evaluations, especially Vision Transformer, whose CER and WER are 23.8% and 18.5% worse than those of our base model on the WD split, and 42.3% and 50.2% worse on the WI split.

4.3 Robustness Evaluation

In this section, we assess the robustness of the models by evaluating them on the WI splits of the adult and children subsets of our word-based dataset. Additionally, we test the performance of models pre-trained on the adult subset against the validation sets of the children subset (Adult2Child), and vice versa (Child2Adult). Pre-trained models from each fold are tested on all validation

sets of the other subset. The mean of all 25 evaluation results is reported as the final result. All models are trained and evaluated using the same configurations as in the previous experiments.

Table 3. Results on the Adult and Children Subsets of Our Word-Based Dataset. We compare our models with other approaches on the WI splits of the adult and children subsets of our word-based dataset, categorized by age group (Adults: ≥ 18 years old; Children: ≤ 12 years old). Models trained on one subset are also evaluated on the other (Adult2Child / Child2Adult).

Models	Adults		Children		Adult2Child		Child2Adult	
	CER	WER	CER	WER	CER	WER	CER	WER
CLDNN	21.62	63.79	28.78	74.06	44.67	86.74	52.32	94.62
CNN+BiLSTM	22.99	67.31	32.11	78.48	45.97	87.25	47.08	92.61
Ours-S	16.22	52.40	22.97	65.47	41.28	81.48	40.69	87.96
ResNet (enc.)	13.74	42.96	18.07	53.64	37.94	78.59	37.89	85.43
MLP-Mixer (enc.)	16.30	50.89	75.29	98.35	41.33	81.94	79.98	99.74
ViT (enc.)	16.42	51.32	32.71	74.88	39.73	81.02	49.74	93.35
ConvNeXt (enc.)	14.63	47.07	24.85	63.85	37.11	79.17	44.48	90.23
SwinV2 (enc.)	14.49	47.48	24.93	66.13	35.97	78.63	42.43	89.53
Ours-B	10.98	36.16	15.00	46.11	35.86	74.86	36.22	82.88

As shown in Table 3, on the adult subset, the CER and WER of our small-version model are 25.0% and 17.9% better than those of CLDNN, which achieves the second-best results. Our base-version model outperforms its closest competitor, ResNet, by 20.1% and 15.8% in CER and WER, respectively. On the children subset, CLDNN and ResNet remain the strongest among the competing models. However, CLDNN is 25.3% and 13.1% worse than our small-version model in CER and WER, while ResNet is 20.5% and 16.3% worse than our base-version model.

Regarding the cross-subset evaluation, our models still perform the best compared to their competitors across all evaluations. After being trained on the larger adult subset, our small-version model performs 7.6% and 6.1% better than its best-performing competitor, CLDNN, in CER and WER on the smaller children subset, while our base-version model performs 17.0% and 14.0% better than its best-performing competitor, ResNet. When trained on the smaller children subset, our small-version model performs 13.6% and 5.0% better than its best-performing competitor, CNN+BiLSTM, in CER and WER on the adult subset, while our base-version model performs 4.4% and 3.0% better than its best-performing competitor, ResNet.

Notably, the MLP-Mixer failed to converge when trained on the children subset, resulting in poor performance in the evaluation on both the adult and children subsets.

4.4 Evaluation on Our Sentence-Based Dataset

In this section, we compare our models with other approaches using the WI splits of our sentence-based dataset. All models are trained and evaluated following the same procedure described in the previous section.

Table 4. Results on Our Sentence-Based Dataset. We compare our models with other approaches on the WI split of our sentence-based dataset.

Models	CER	WER	#Params	MACs
CLDNN	17.47	59.17	0.75M	1.17B
CNN+BiLSTM	18.94	66.25	0.41M	0.61B
Ours-S	13.22	48.75	0.54M	0.32B
ResNet (enc.)	8.20	28.74	3.97M	2.37B
MLP-Mixer (enc.)	75.14	100.00	15.71M	8.04B
ViT (enc.)	10.57	37.35	3.72M	1.93B
ConvNeXt (enc.)	9.48	34.72	3.87M	2.40B
SwinV2 (enc.)	9.06	33.44	3.89M	2.41B
Ours-B	6.78	24.63	3.90M	2.40B

As shown in Table 4, our models achieve the lowest error rates. The small version reaches a CER of 13.22% and a WER of 48.75%, which are 24.3% and 17.6% better than the second-best model, CLDNN, while also consuming the least computational resources. The base version achieves a CER of 6.78% and a WER of 24.63%, outperforming the second-best model, ResNet, by 20.9% and 16.7%, respectively.

Notably, the MLP-Mixer again failed to converge, resulting in a WER of 100% on this dataset, despite having a significantly larger number of parameters and higher computational cost than the other approaches. Vision Transformer, another global attention-based model, performs the second worst, with a CER of 10.57% and a WER of 37.35%, although it has the smallest model size and the lowest computational cost.

Furthermore, we analyze the errors made by the base version of our model on the WI split of our sentence-based dataset. As shown in Appendix C, substitution remains the primary error type, although deletions occur more frequently than in the word-based dataset. In addition to confusion between uppercase and lowercase versions of the same letter, errors caused by extreme data imbalance are more prominent, especially for characters like "Q". Some characters are frequently misrecognized as "Q", which appears very rarely in the dataset, as illustrated in Appendix B.

4.5 Ablation Study

In this section, we conduct an ablation study on the WI split of our word-based dataset. Since our method is based on CLDNN, we evaluate the performance

improvements achieved through a series of incremental changes, including an optimized training procedure, data augmentation, architectural enhancements, and model size scaling.

Table 5. Ablation Study Results. We evaluate the performance of our model on the WI split of our dataset, incorporating incremental modifications based on CLDNN.

Models	CER	WER	#Params	MACs
CLDNN	19.05	60.20	0.75M	291M
+ Optimized training	17.81	56.54	0.75M	291M
+ Data augmentation	17.22	55.60	0.75M	291M
+ Reverse dimension order	16.09	53.62	0.92M	214M
+ Embedding layer	19.04	58.52	0.64M	99M
+ Separable convolution	18.00	56.59	0.55M	81M
+ Multi-scale convolution	18.15	56.56	0.55M	81M
+ Instance normalization	15.60	51.31	0.55M	81M
+ GELU	15.34	50.88	0.55M	81M
+ Remove hidden layer (Ours-S)	15.29	50.70	0.53M	79M
+ Scale up (Ours-B)	9.44	32.17	3.89M	600M

As shown in Table 5, we first employ an optimized training pipeline and data augmentation, which improve performance by 9.6% and 7.6% on CER and WER, respectively, without any modifications to the model architecture. Reversing the dimension order of each stage from 512, 256, 128 to 128, 256, 512 slightly increases model size but reduces both error rates and computational cost. Using embedding layers with smaller dimensions of 64, 128, and 256 increases the CER from 16.09% to 19.04% and the WER from 53.62% to 58.52%, but reduces the number of parameters and MACs by 30.4% and 53.7%, respectively.

A combination of micro modifications to the convolutional block, including depthwise-dilated separable convolution, multi-scale convolution, instance normalization, and GELU, significantly improves performance to 15.34% CER and 50.88% WER, representing gains of 19.4% and 13.1%, respectively. Among these changes, instance normalization contributes additional improvements of 14.0% in CER and 9.3% in WER, building on the gains already achieved by depthwise-dilated separable convolution and multi-scale convolution.

In addition to modifications to the convolutional encoder, we removed the hidden layers of CLDNN, resulting in the small version of our model. It achieves 15.29% CER and 50.70% WER, which are 19.7% and 15.8% better than CLDNN, while using only 0.53M parameters and 79M MACs, which are 29.3% and 72.9% less than those of CLDNN. We also scale up the model by using three convolutional blocks per stage, encoder dimensions of 128, 256, and 512, a BiLSTM with 128 hidden units, and three BiLSTM layers. This results in the base version of our model, which achieves 9.44% CER and 32.17% WER, representing 50.4% and 46.6% improvements over CLDNN, using 3.89M parameters and 600M MACs, which are $5.2\times$ and $2.1\times$ those of CLDNN.

5 Discussion

5.1 Efficiency

Across all evaluations, we demonstrate the strong efficiency of our models, particularly the small version, which is designed for deployment on edge devices. It achieves significantly lower error rates compared to other IMU-based HWR approaches while using only 53.3% of the parameters and 27.1% of the computational cost of CLDNN. This efficiency can greatly enhance the user experience on capable edge devices by providing better recognition accuracy without incurring communication latency to remote servers.

The base version, in contrast, is designed for server-side deployment, prioritizing higher accuracy by processing raw IMU signals with more parameters. Although it is outperformed by ResNet on the WD split, our base-version model surpasses all competitors on the WI split while maintaining a comparable model size and computational cost, demonstrating a strong balance between efficiency and performance.

5.2 Robustness

Handwriting styles vary greatly among individuals, posing significant challenges for HWR. Since it is unrealistic to train a model on data that captures every possible handwriting style, evaluating models on WI datasets provides a more practical and meaningful measure of performance than WD or random-split datasets. WI evaluation ensures that handwriting styles in the training and test sets do not overlap, more accurately reflecting real-world scenarios where a model must generalize to unseen writers. Our models consistently outperform all competitors across all WI splits, demonstrating a strong ability to extract robust handwriting features that generalize effectively across diverse writing styles.

Children are beginners in handwriting, and their writing styles differ significantly from those of adults, making HWR more challenging. However, children are also an important user group for HWR systems, given the frequent handwriting activities in educational settings. Therefore, developing a solution that performs well for both adults and children is essential to the success of an HWR system. Our robustness evaluation shows that our models outperform all competitors on both adult and child subsets. Moreover, the results from the cross-subset evaluation suggest that our models learn more generalizable representations, as they maintain strong performance even when trained and validated on different age groups.

Additionally, noise from the writing surface and sensors is common in HWR systems and can potentially degrade performance, limiting the environments in which these systems can be used. In our ablation study, we demonstrate that using data augmentations such as AddNoise, Drift, and Dropout to simulate noise significantly improves the performance of our HWR system. This proves that data augmentation can be an effective solution for handling noise and improving the system’s robustness.

5.3 Flexibility

Due to the nature of handwriting, IMU handwriting signals always vary in size. Models like ViT and Swin Transformers, limited by positional embeddings or shifting mechanisms, require suboptimal compromises such as padding or truncating to process inputs of different sizes. However, padding increases meaningless computational overhead, while truncating can lead to the loss of important information. In contrast, the CNN-BiLSTM design processes inputs of any size without resizing, enabling efficient computation and adaptability. Thus, approaches that can process inputs of varying sizes are the way to go for IMU-based HWR.

6 Conclusion & Outlook

In conclusion, our experiments demonstrate that the proposed model consistently outperforms competitors on WI datasets, showcasing strong efficiency, robustness, and flexibility in HWR. However, there is still room for improvement.

The design and evaluation of our approach are limited by the dataset. The dataset is highly imbalanced, with certain characters appearing too infrequently to be meaningful. Additionally, we have not yet investigated whether specific error patterns could provide insights for further reducing the error rate. By identifying and addressing semantic errors in the data, such as typos or misalignments between IMU signals and text labels, we could curate the dataset to improve its quality. This refinement could enhance the performance of HWR systems, produce more reliable results, and offer deeper insights into the remaining challenges in handwriting recognition.

Additionally, although the models show strong performance on our sentence-based dataset, character-level recognition remains a suboptimal approach for leveraging contextual information. It results in a pattern-matching solution that lacks an understanding of language semantics from the IMU signals. This limitation could potentially be addressed by incorporating natural language processing techniques into HWR systems.

References

1. Alemayoh, T.T., Shintani, M., Lee, J.H., Okamoto, S.: Deep-learning-based character recognition from handwriting motion data captured using imu and force sensors. *Sensors* **22**(20) (2022). <https://doi.org/10.3390/s22207840>, <https://www.mdpi.com/1424-8220/22/20/7840>
2. Carbune, V., Gonnet, P., Deselaers, T., Rowley, H.A., Daryin, A., Calvo, M., Wang, L.L., Keysers, D., Feuz, S., Gervais, P.: Fast multi-language lstm-based online handwriting recognition. *International Journal on Document Analysis and Recognition (IJDAR)* **23**(2), 89–102 (Jun 2020). <https://doi.org/10.1007/s10032-020-00350-4>, <https://doi.org/10.1007/s10032-020-00350-4>
3. Choi, S.d., Lee, A.S., Lee, S.y.: On-line handwritten character recognition with 3d accelerometer. In: 2006 IEEE International Conference on Information Acquisition. pp. 845–850 (2006). <https://doi.org/10.1109/ICIA.2006.305842>

4. Dosovitskiy, A., Beyer, L., Kolesnikov, A., Weissenborn, D., Zhai, X., Unterthiner, T., Dehghani, M., Minderer, M., Heigold, G., Gelly, S., Uszkoreit, J., Houshy, N.: An image is worth 16x16 words: Transformers for image recognition at scale. In: International Conference on Learning Representations (2021), <https://openreview.net/forum?id=YicbFdNTTy>
5. Graves, A., Fernández, S., Gomez, F., Schmidhuber, J.: Connectionist temporal classification: labelling unsegmented sequence data with recurrent neural networks. In: Proceedings of the 23rd International Conference on Machine Learning. pp. 369–376. ICML '06, Association for Computing Machinery, New York, NY, USA (2006). <https://doi.org/10.1145/1143844.1143891>, <https://doi.org/10.1145/1143844.1143891>
6. Hassan, E., Tarek, H., Hazem, M., Bahnacy, S., Shaheen, L., Elashmwai, W.H.: Medical prescription recognition using machine learning. In: 2021 IEEE 11th Annual Computing and Communication Workshop and Conference (CCWC). pp. 0973–0979 (2021). <https://doi.org/10.1109/CCWC51732.2021.9376141>
7. He, K., Zhang, X., Ren, S., Sun, J.: Deep residual learning for image recognition. In: Proceedings of the IEEE Conference on Computer Vision and Pattern Recognition (CVPR) (June 2016)
8. Jeen-Shing, W., Yu-Liang, H., Cheng-Ling, C.: Online handwriting recognition using an accelerometer-based pen device. In: Proceedings of the 2nd International Conference on Advances in Computer Science and Engineering (CSE 2013). pp. 231–234. Atlantis Press (2013/07). <https://doi.org/10.2991/cse.2013.52>, <https://doi.org/10.2991/cse.2013.52>
9. Liu, Z., Hu, H., Lin, Y., Yao, Z., Xie, Z., Wei, Y., Ning, J., Cao, Y., Zhang, Z., Dong, L., Wei, F., Guo, B.: Swin transformer v2: Scaling up capacity and resolution. In: International Conference on Computer Vision and Pattern Recognition (CVPR) (2022)
10. Liu, Z., Lin, Y., Cao, Y., Hu, H., Wei, Y., Zhang, Z., Lin, S., Guo, B.: Swin transformer: Hierarchical vision transformer using shifted windows. In: Proceedings of the IEEE/CVF International Conference on Computer Vision (ICCV) (2021)
11. Liu, Z., Mao, H., Wu, C.Y., Feichtenhofer, C., Darrell, T., Xie, S.: A convnet for the 2020s. Proceedings of the IEEE/CVF Conference on Computer Vision and Pattern Recognition (CVPR) (2022)
12. Lopez-Rodriguez, P., Avina-Cervantes, J.G., Contreras-Hernandez, J.L., Correa, R., Ruiz-Pinales, J.: Handwriting recognition based on 3d accelerometer data by deep learning. Applied Sciences **12**(13) (2022). <https://doi.org/10.3390/app12136707>, <https://www.mdpi.com/2076-3417/12/13/6707>
13. Meißl, F., Eibensteiner, F., Petz, P., Langer, J.: Online handwriting recognition using lstm on microcontroller and imu sensors. In: 2022 21st IEEE International Conference on Machine Learning and Applications (ICMLA). pp. 999–1004 (2022). <https://doi.org/10.1109/ICMLA55696.2022.00167>
14. Ott, F., Rügamer, D., Heublein, L., Hamann, T., Barth, J., Bischl, B., Mutschler, C.: Benchmarking online sequence-to-sequence and character-based handwriting recognition from imu-enhanced pens. Int. J. Doc. Anal. Recognit. **25**(4), 385–414 (Dec 2022). <https://doi.org/10.1007/s10032-022-00415-6>, <https://doi.org/10.1007/s10032-022-00415-6>
15. Pontart, V., Bidet-Ildei, C., Lambert, E., Morisset, P., Flouret, L., ALAMARGOT, D.: Influence of handwriting skills during spelling in primary and lower secondary grades. Frontiers in Psychology **4** (2013). <https://doi.org/10.3389/fpsyg.2013.00818>, <https://www.frontiersin.org/journals/psychology/articles/10.3389/fpsyg.2013.00818>

16. Seuret, M., van der Loop, J., Weichselbaumer, N., Mayr, M., Molnar, J., Hass, T., Christlein, V.: Combining ocr models for reading early modern books. In: Fink, G.A., Jain, R., Kise, K., Zanibbi, R. (eds.) Document Analysis and Recognition - ICDAR 2023. pp. 342–357. Springer Nature Switzerland, Cham (2023)
17. Skar, G.B., Lei, P.W., Graham, S., Aasen, A.J., Johansen, M.B., Kvistad, A.H.: Handwriting fluency and the quality of primary grade students' writing. *Reading and Writing* **35**(2), 509–538 (2022). <https://doi.org/10.1007/s11145-021-10185-y>, <https://doi.org/10.1007/s11145-021-10185-y>
18. Tolstikhin, I.O., Houlsby, N., Kolesnikov, A., Beyer, L., Zhai, X., Unterthiner, T., Yung, J., Steiner, A., Keysers, D., Uszkoreit, J., Lucic, M., Dosovitskiy, A.: Mlp-mixer: An all-mlp architecture for vision. In: Ranzato, M., Beygelzimer, A., Dauphin, Y., Liang, P., Vaughan, J.W. (eds.) *Advances in Neural Information Processing Systems*. vol. 34, pp. 24261–24272. Curran Associates, Inc. (2021)
19. Vaswani, A., Shazeer, N., Parmar, N., Uszkoreit, J., Jones, L., Gomez, A.N., Kaiser, L.u., Polosukhin, I.: Attention is all you need. In: Guyon, I., Luxburg, U.V., Bengio, S., Wallach, H., Fergus, R., Vishwanathan, S., Garnett, R. (eds.) *Advances in Neural Information Processing Systems*. vol. 30. Curran Associates, Inc. (2017)
20. Wehbi, M., Hamann, T., Barth, J., Eskofier, B.: Digitizing handwriting with a sensor pen: A writer-independent recognizer. In: 2020 17th International Conference on Frontiers in Handwriting Recognition (ICFHR). pp. 295–300 (2020). <https://doi.org/10.1109/ICFHR2020.2020.00061>
21. Wehbi, M., Hamann, T., Barth, J., Kaempf, P., Zanca, D., Eskofier, B.: Towards an imu-based pen online handwriting recognizer. In: Lladós, J., Lopresti, D., Uchida, S. (eds.) *Document Analysis and Recognition – ICDAR 2021*. pp. 289–303. Springer International Publishing, Cham (2021)

A Visualization of Data Augmentation

As shown in the visualization of data augmentations in Figure 3, AddNoise, Drift, and Dropout are applied in a multiplicative manner to ensure that the augmentation magnitude is neither overshadowed by the original signal nor dominates it.

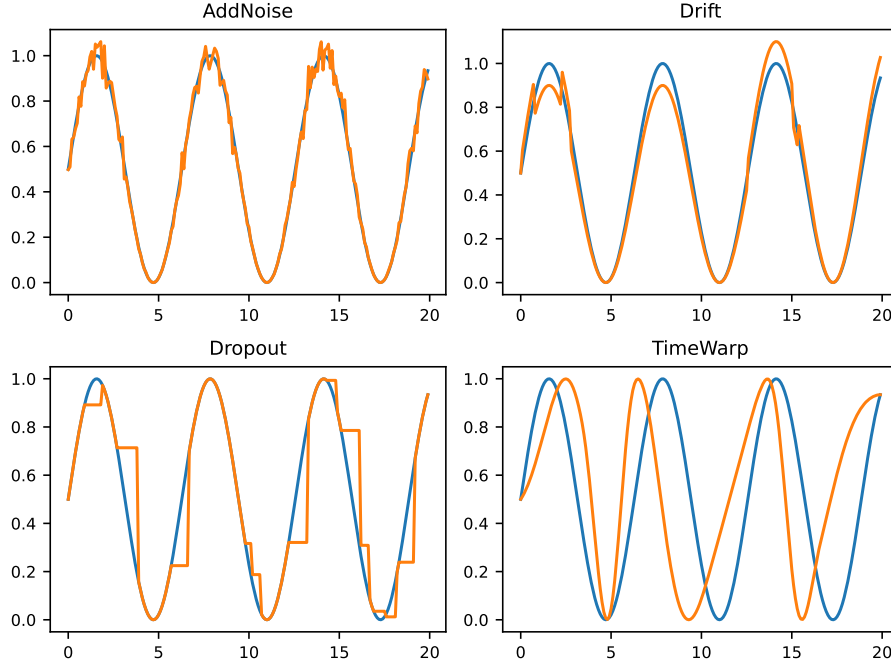


Fig. 3. Data augmentation. Examples of sine signals with different data augmentation techniques applied, where the blue curve represents the original sine signal and the orange curve represents the augmented signal.

B Visualization of Character and Length Distribution

As shown in the character distributions of both the word-based (Figure 4) and sentence-based (Fig.5) datasets, the distribution is dominated by lowercase letters, particularly "e", "n", and "r", due to the nature of English and German. Although the sentence-based dataset includes sentences composed exclusively of numbers and symbols, their overall frequency remains very low. Additionally, the space character, which plays a crucial role in sentence structure, has the second-highest frequency among all characters.

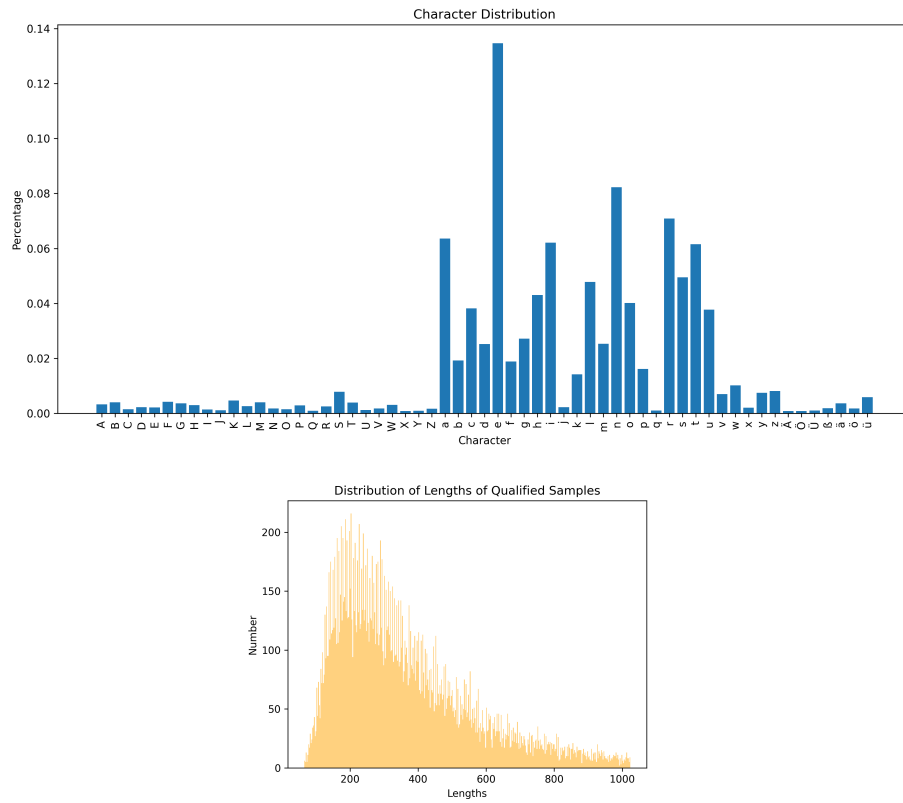


Fig.4. Character and sequence length distributions in the word-based dataset. The top plot shows the frequency of each character; the bottom plot shows the distribution of sequence lengths.

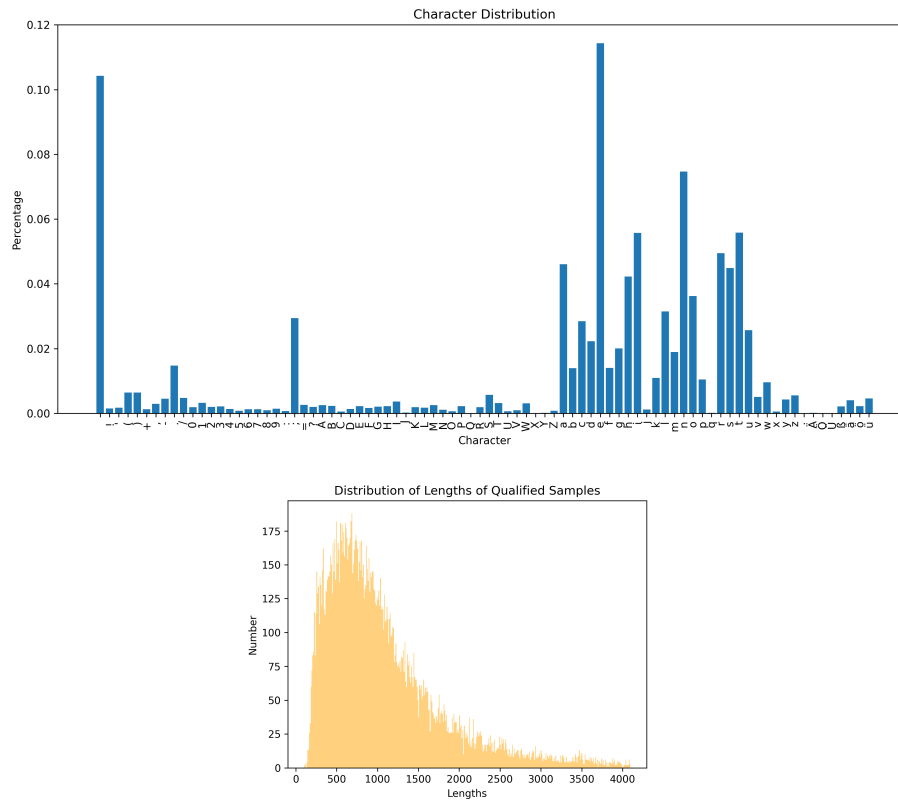


Fig. 5. Character and sequence length distributions in the sentence-based dataset. The top plot shows the frequency of each character; the bottom plot shows the distribution of sequence lengths.

C Visualization of Substitution Error Rates

Figure 6 shows the substitution error matrix of our base-version model on the first fold of the WI split of the word-based dataset.

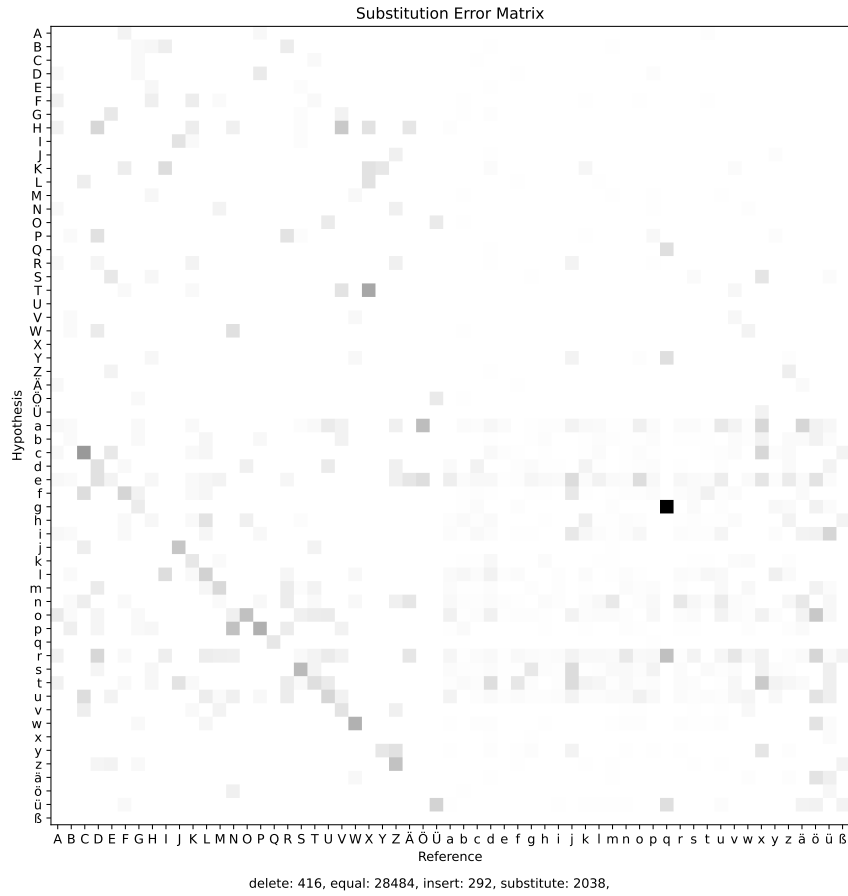


Fig. 6. Substitution Errors on Word-Based Dataset. Substitution errors made by the base version of our model on the WI split of our word-based dataset are visualized. Darker shades indicate higher error rates.

Figure 7 presents the substitution error matrix of the same model on the first fold of the WI split of the sentence-based dataset.

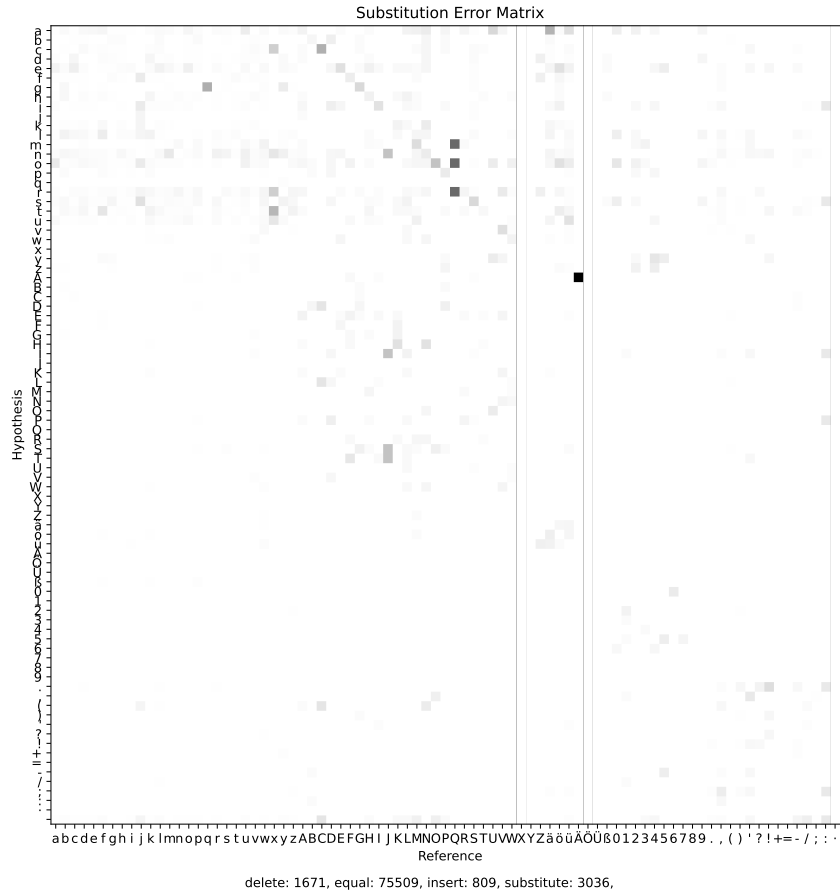


Fig. 7. Substitution Errors on Sentence-Based Dataset. Substitution errors made by the base version of our model on the WI split of our sentence-based dataset are visualized.